

Computation of Local Volatilities from Regularized Dupire Equations

Martin Hanke* Elisabeth Rösler

Fachbereich Mathematik, Johannes Gutenberg-Universität
55099 Mainz, Germany

June 11, 2004

Abstract

We propose a new method to calibrate the local volatility function of an asset from observed option prices of the underlying. Our method is initialized with a preprocessing step in which the given data are smoothed using cubic splines before they are differentiated numerically. In a second step the Dupire equation is rewritten as a linear equation for a rational expression of the local volatility. This equation is solved with Tikhonov regularization, using some discrete gradient approximation as penalty term. We show that this procedure yields local volatilities which appear to be qualitatively correct.

1 Introduction

We study the *inverse problem of option pricing* which is concerned with the approximation of the so-called *volatility function* σ of an underlying asset with price $S = S(t)$, given by the (lognormal) stochastic process

$$dS/S = \mu dt + \sigma dW, \quad t > t_0, \quad S(t_0) = S_0, \quad (1.1)$$

with drift μ and normalized Brownian motion W . Here, the volatility may depend on time and on the underlying asset price, i.e., $\sigma = \sigma(t, S)$.

A European *call option* on the underlying with maturity date T and strike X gives the right to buy one unit of the asset at time T and price X . Assuming that (1.1) holds true, the celebrated Black-Scholes model determines the fair price $u = u(t, x; T, X)$ of this option at time t given an asset price x at this time, from the solution of the parabolic differential equation

$$\begin{aligned} -u_t &= \frac{1}{2}\sigma^2(t, x)x^2u_{xx} + rxu_x - ru, & t < T, \quad x > 0, \\ u(T, x; T, X) &= \max\{x - X, 0\}, & x \geq 0, \end{aligned} \quad (1.2)$$

*corresponding author

with boundary values

$$u(t, 0; T, X) = 0, \quad \lim_{x \rightarrow \infty} \frac{u(t, x; T, X)}{x} = 1, \quad t < T. \quad (1.3)$$

If the volatility σ is known, this boundary value problem is well-posed and allows the stable computation of the option price. However, in practice the volatility is not known explicitly, hence the importance of the aforementioned inverse problem, where one tries to estimate or reconstruct the volatility function from observed market prices $u(t_0, S_0; T, X)$ at a *fixed time* t_0 given the *fixed price* $S_0 = S(t_0)$ of the underlying.

Inverse problems in diffusion processes have a certain tradition in the mathematical community, cf., e.g., the conference proceedings [4], albeit in those problems data are typically given for one particular solution with fixed boundary and initial data. In contrast, we are given here data from different solutions of (1.2) corresponding to different initial conditions (1.3) using different strikes and maturity dates. Nevertheless, these inverse problems have in common that the vast majority of them is ill-posed, and some kind of regularization is required for a stable solution.

We refer to Crépey [1] for an up-to-date survey of methods to solve the inverse problem of option pricing. Most of them use some *output least squares approach* and minimize a (nonlinear) least squares functional with a Tikhonov-type penalty term for regularization. However, as first observed by Dupire [2], there is an alternative and more direct way to obtain the volatility function, and which is based on the Fokker-Planck equation associated with the diffusion process (1.1). According to that we can consider the option price $u = u(t_0, S_0; T, X)$ as a function of T and X which satisfies the differential equation

$$\begin{aligned} u_T &= \frac{1}{2} \sigma^2(T, X) X^2 u_{XX} - r X u_X, & T > t_0, \quad X > 0, \\ u(t_0, S_0; t_0, X) &= \max\{S_0 - X, 0\}, & X \geq 0, \end{aligned} \quad (1.4)$$

with boundary values

$$u(t_0, S_0; T, 0) = S_0, \quad \lim_{X \rightarrow \infty} u(t_0, S_0; T, X) = 0. \quad (1.5)$$

Note that we can solve (1.4) for the volatility

$$\sigma(T, X) = \left(\frac{2(u_T + r X u_X)}{X^2 u_{XX}} \right)^{1/2}, \quad (1.6)$$

where all derivatives of u on the right-hand side of (1.6) are to be evaluated at $(t_0, S_0; T, X)$, and therefore can, in principle, be computed from the given data.

Despite its simplicity, this approach has severe practical shortcomings which reflect the ill-posedness of the problem. First, financial markets typically allow only few and prefixed maturity dates, and just a discrete sample of strikes are on sell, too; therefore some sort of numerical differentiation is required to evaluate the fraction in (1.6). Second, the geometric Brownian motion (1.1) and the

Black-Scholes equation (1.2) are just models of real market dynamics, so that (1.6) is at best an approximate identity.

In fact, real option prices (for fixed t_0 and S_0) are typically

- monotonically decreasing and convex in X , and
- monotonically increasing in T ,

and this implies in particular that the denominator of (1.6) is usually positive; however, positivity of the numerator may not be an obvious property for real data. Therefore it can easily happen that the computed fractions in (1.6) change sign, and taking the square root to obtain σ is prohibited. Even if the fraction remains finite and positive the volatility functions computed from (1.6) exhibit rough oscillations, if the data have not been preprocessed properly, cf., e.g., the examples in [1].

It is the purpose of this paper to restore stability for this approach by adopting a technique from [6] to the present context. Basically, this amounts to rewrite (1.4) as a linear system of equations for the unknown volatilities, and to use Tikhonov regularization with a discrete H^1 penalty term to obtain a smooth solution of this system. This approach still requires numerical differentiation of the discrete data, and we use a smooth cubic spline interpolation for this, cf. Section 2. This can be interpreted as a data preprocessing step which adds some more regularization to our implementation. In Section 3 we describe in detail the modifications of (1.6) that we introduce to obtain a smooth approximate volatility function. To justify our approach we present numerical results in Section 4, both for synthetic as well as real data sets. The reconstructions of the volatility functions appear to be qualitatively correct, and at the same time, the whole algorithm is extremely fast: there is just one linear matrix equation, but no partial differential equation to be solved.

2 Numerical differentiation of the available data

In practice options are only sold for very few maturities: Typically, only one preassigned day per month qualifies for a maturity time, and from those maturities only few are actually on sale. We denote them by T_1, \dots, T_m . For each T_i a certain number of strikes is available, and we shall assume for simplicity that the smallest and largest of these, X_* and X^* , are the same for each maturity. For our main example, the bullets in Figure 1 show the given combinations of T and X for options on the S&P500 index from April 17, 2002 [9], where $t_0 = 0$, $S_0 = 1127.9$, $X_* = 1025$ and $X^* = 1200$ (time units are days, option units are index points).

To evaluate (1.6) we need to differentiate these discrete data twice with respect to the strike variable X . Following Reinsch [10], see also [7], we compute, for each maturity T_i , $i = 1, \dots, m$, a smoothing natural cubic spline u_i such that

$$\sum_X |u_i(X) - u(t_0, S_0; T_i, X)|^2 + \lambda \|u_i''\|_{\mathcal{L}^2}^2 \quad (2.1)$$

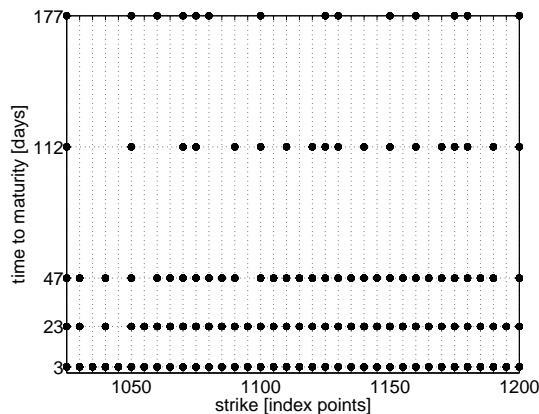


Figure 1: Available data for the S&P500 index from April 17, 2002

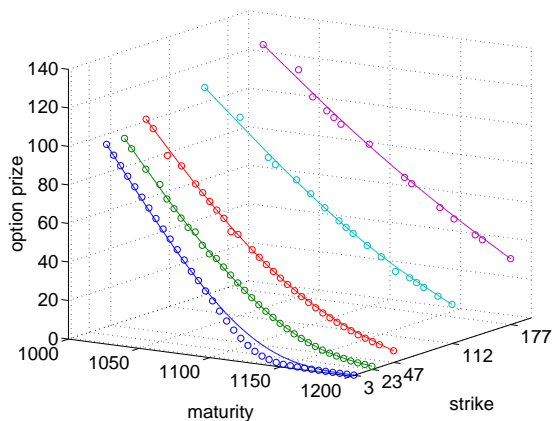


Figure 2: Smooth interpolation of the S&P500 index data

is minimized. While the boundary values $u_i(X_*)$ and $u_i(X^*)$ are prescribed by the data, the sum in (2.1) runs over all interior strikes X which are available for the maturity T_i ; the \mathcal{L}^2 -norm refers to the interval $[X_*, X^*]$. The positive parameter λ depends on i and is known as Lagrange or regularization parameter. Once the cubic splines u_i are determined they can easily be differentiated analytically to compute approximations of u_X and u_{XX} wherever needed. Figure 2 shows the given option prices (as circles), and the result of the smooth interpolation (the solid lines).

We emphasize that alternative techniques for the numerical differentiation of the data exist (cf., e.g., the references in [7]) and can in principle be employed as well. An advantage of the above approach is the well-known fact that the cubic spline is differentiable twice, and has small curvature. Another advantage is that the spline functions can be evaluated at any point in the interval $[X_*, X^*]$,

a property that we will use later on.

Of course, the regularization involved in (2.1) is a crucial issue, and we briefly comment on how to determine an appropriate regularization parameter λ . With a standard strategy, the so-called *discrepancy principle*, this parameter is chosen such that the sum of squares in (2.1) equals the data uncertainty (which can, for example, be estimated from the bid-ask spread of the market) times the number of data samples. We refer to [7] for references and an error analysis of this procedure. In our implementation we have used an alternative approach for choosing λ based on the so-called *L-curve criterion*, cf., e.g., [3, Section 4.5]. For this criterion one computes the minimizers $u_{i,\lambda}$ of (2.1) for a significant range of regularization parameters, and evaluates the corresponding residual and solution norms in (2.1):

$$\rho(\lambda) = \sum_X |u_{i,\lambda}(X) - u(t_0, S_0; T_i, X)|^2, \quad \nu(\lambda) = \|u''_{i,\lambda}\|_{\mathcal{L}^2}^2.$$

The curve $(\rho(\lambda), \nu(\lambda))$ often exhibits an L-shaped corner when plotted in a doubly logarithmic scale, and regularization parameters corresponding to points just to the right of that corner have proved useful in various applications. We refer to Figure 3 for two such L-curves associated with the data smoothing problem (2.1): from left to right the regularization parameter is increasing in the two curves. Both of them have distinct L-shaped corners. However, it turns out that in certain cases we need to impose somewhat more regularization than suggested by the original L-curve criterion to achieve positivity of $u_{i,\lambda}$ and its second derivative. To illustrate this point we have marked with circles those points on the curves for which these two functions are positive. (In our code we sample each curve for $\lambda = 10^{\nu/2}$ with integer $\nu \in \{-14, \dots, 2\}$; the solid lines in Figure 3 are obtained by subsampling and serve for illustration only.) Out of these points, the one which is nearest to the corner but still to its right, yields our parameter of choice; these points are marked with bullets in the figure.

Differentiation with respect to time is less delicate because of the relatively large time gaps. While this implies that the numerical differentiation cannot be very accurate, it also means that lack of stability is not really an issue here. Therefore we can use simple difference schemes to approximate the time derivatives at the maturity times. More precisely, we use centered differences at the inner maturities T_2, \dots, T_{m-1} , and one-sided differences at the extremal maturities T_1 and T_m . Note that the maturities are not equispaced, so that the appropriate central difference quotient is

$$u_T(X_i, T_j) \approx \frac{1}{\tau_j + \tau_{j+1}} \left(\frac{\tau_j}{\tau_{j+1}} u_{j+1}(X_i) + \left(\frac{\tau_{j+1}}{\tau_j} - \frac{\tau_j}{\tau_{j+1}} \right) u_j(X_i) - \frac{\tau_{j+1}}{\tau_j} u_{j-1}(X_i) \right),$$

with $\tau_j = T_j - T_{j-1}$, $j = 2, \dots, m-1$.

3 Solving for the unknown volatility function

We choose a rectangular grid Δ with equispaced grid points at the abscissa $X_* = X_1 < X_2 < \dots < X_n = X^*$ in X direction (in our implementation we

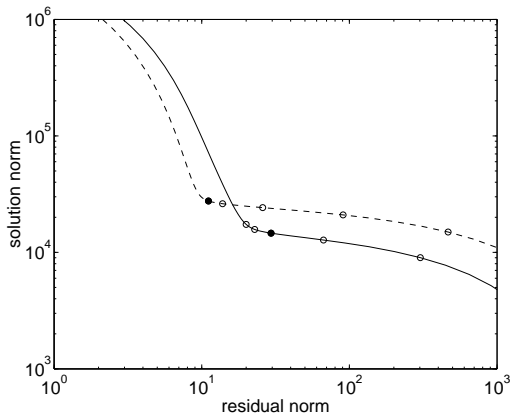


Figure 3: L-curves for two of the second derivative computations

use one grid point per index point, i.e. much more grid points than the number of strikes we have) and ordinates in time at $T_0 = t_0$ and at each maturity T_i , $i = 1, \dots, m$, measured in years. Then we associate unknown values

$$z_{ij} = \sigma^2(T_i, X_j), \quad i = 0, \dots, m, \quad j = 1, \dots, n,$$

of the squared volatility function with all points $(T_i, X_j) \in \Delta$, as well as corresponding values d_{ij} and b_{ij} for the denominator and the numerator of the fraction in (1.6), respectively. While the latter can be computed using numerical derivatives as specified in Section 2 when $i > 0$, we set them to zero for $i = 0$. We stack all those values in one-dimensional vectors \mathbf{z} , \mathbf{d} , and $\mathbf{b} \in \mathbb{R}^N$, $N = (m + 1)n$, using a standard lexicographical ordering (with all abscissa for a single maturity in consecutive, increasing, order).

The key idea of our first approach is to consider the expression in (1.6) as a linear system

$$D\mathbf{z} \approx \mathbf{b}, \quad (3.1)$$

where D is the diagonal matrix whose diagonal coincides with \mathbf{d} . Note that, by construction, those equations in (3.1) corresponding to grid points with $T_0 = t_0$ are trivially correct, although the corresponding entries of \mathbf{z} are not uniquely determined. But even without these trivial equations the matrix D is singular because we use natural cubic splines u_i for the interpolation, and hence the denominators of (1.6) vanish when $X = X_1$ or $X = X_n$. In the vicinity of these points the entries of \mathbf{d} are still tiny so that D happens to be relatively ill-conditioned in general. Finally, although D is nonnegative by construction the system (3.1) may not have a nonnegative solution because of possible sign changes in \mathbf{b} .

For these reasons the linear system (3.1) needs to be regularized to obtain reasonable approximations of \mathbf{z} . We use Tikhonov regularization (cf., e.g., [3,

Chapter 5]) which amounts to minimize

$$\|D\mathbf{z} - \mathbf{b}\|_2^2 + \alpha \|L\mathbf{z}\|_2^2 \quad (3.2)$$

over $\mathbf{z} \in \mathbb{R}^N$ for some appropriate regularization parameter $\alpha > 0$. Here, $\|\cdot\|_2$ denotes the Euclidean norm. Care has to be taken in the choice of L . For example, the identity matrix $L = I$ will in general not yield nonnegative solutions \mathbf{z} , either, because the minimization of (3.2) is equivalent to solving the linear system

$$(D^2 + \alpha L^T L)\mathbf{z} = D\mathbf{b}, \quad (3.3)$$

and with $L = I$ the system matrix in (3.3) is a diagonal matrix with positive diagonal, but the right-hand side of (3.3) has the same sign changes as \mathbf{b} .

Rather, we recommend to use finite difference approximations to define a discrete gradient operator L . More precisely, we choose

$$L = \begin{bmatrix} I_{m+1} \otimes L_X \\ L_T \otimes I_n \end{bmatrix}, \quad (3.4)$$

where $L_X \in \mathbb{R}^{n-1,n}$ and $L_T \in \mathbb{R}^{m,m+1}$ are given by

$$L_X = \begin{bmatrix} -1 & 1 & & & \\ & -1 & 1 & & \\ & & \ddots & \ddots & \\ & & & -1 & 1 \end{bmatrix}, \quad L_T = \begin{bmatrix} -1/\tau_1 & 1/\tau_1 & & & \\ & -1/\tau_2 & 1/\tau_2 & & \\ & & \ddots & \ddots & \\ & & & -1/\tau_m & 1/\tau_m \end{bmatrix},$$

with $\tau_i = T_i - T_{i-1}$ as above, and $(m+1, m+1)$ and (n, n) identity matrices I_{m+1} and I_n , respectively. The symbol \otimes denotes the *Kronecker product* of two matrices, i.e., if $A = [a_{ij}] \in \mathbb{R}^{k,l}$ and B is any matrix then $A \otimes B$ is the block matrix

$$A \otimes B = \begin{bmatrix} a_{11}B & a_{12}B & \dots & a_{1l}B \\ a_{21}B & a_{22}B & \dots & a_{2l}B \\ \vdots & & & \vdots \\ a_{k1}B & a_{k2}B & \dots & a_{kl}B \end{bmatrix}.$$

Although L of (3.4) has the nontrivial null space of all constant vectors, the matrix $D^2 + \alpha L^T L$ in (3.3) is always nonsingular for positive α . One advantage of using this particular L over the identity matrix consists in a coupling of the individual values $\sigma^2(T_i, X_j)$ in \mathbf{z} obtained this way. In particular, this coupling also includes the components $\sigma^2(t_0, X_j)$ which are otherwise undetermined by (1.4). Furthermore, it turns out that we obtain positive solutions \mathbf{z} of (3.3) provided that α is sufficiently large: this is the content of the following result.

Theorem 1. *Let \mathbf{d} and \mathbf{b} be as above, and assume that $\sum d_{ij}b_{ij} > 0$. Denote by $\mathbf{1}$ the constant vector of all ones in \mathbb{R}^N , and let \mathbf{z}_α be the solution of (3.3). Then*

$$\mathbf{z}_\alpha \rightarrow \frac{\sum d_{ij}b_{ij}}{\sum d_{ij}^2} \mathbf{1}, \quad \alpha \rightarrow \infty.$$

Proof. We make use of the *generalized singular value decomposition* of the matrix pair (L, D) , cf., e.g., Golub and Van Loan [5], i.e.,

$$L = UCX^{-1}, \quad D = V SX^{-1}, \quad (3.5)$$

with orthogonal matrices U and V , a nonsingular matrix $X \in \mathbb{R}^{N \times N}$, and two diagonal matrices C and S from $\mathbb{R}^{N \times N}$ with nonnegative diagonal entries c_i and s_i , $i = 1, \dots, N$, respectively. We denote the columns of V by $\mathbf{v}_1, \dots, \mathbf{v}_N$ and the columns of X by $\mathbf{x}_1, \dots, \mathbf{x}_N$, i.e.,

$$V = [\mathbf{v}_1, \dots, \mathbf{v}_N], \quad X = [\mathbf{x}_1, \dots, \mathbf{x}_N];$$

each of these vectors belongs to \mathbb{R}^N . Since the ranks of L and C coincide, exactly one diagonal entry of C is zero, c_N say. Accordingly, the last column of X can be chosen to be $\mathbf{x}_N = \mathbf{1}$. Moreover, we have

$$\mathbf{d} = D\mathbf{1} = D\mathbf{x}_N = s_N\mathbf{v}_N \quad \text{and} \quad \mathbf{v}_N^T \mathbf{b} = \mathbf{d}^T \mathbf{b} / s_N, \quad (3.6)$$

and since \mathbf{v}_N has unit length,

$$s_N^2 = \|\mathbf{d}\|_2^2. \quad (3.7)$$

Inserting (3.5) into (3.3) and using the symmetry of $D = D^T$ we obtain

$$\begin{aligned} \mathbf{z}_\alpha &= (D^2 + \alpha L^T L)^{-1} D \mathbf{b} = X(S^2 + \alpha C^2)^{-1} X^T X^{-T} S V^T \mathbf{b} \\ &= \sum_{i=1}^N \mathbf{v}_i^T \mathbf{b} \frac{s_i}{s_i^2 + \alpha c_i^2} \mathbf{x}_i \end{aligned}$$

because U and V are orthogonal matrices, and hence, $U^T U$ and $V^T V$ equal the $N \times N$ identity matrix. Letting α go to infinity, only the last term of this sum remains because $c_i \neq 0$ for $i \neq N$, so that

$$\lim_{\alpha \rightarrow \infty} \mathbf{z}_\alpha = \frac{\mathbf{v}_N^T \mathbf{b}}{s_N} \mathbf{1}.$$

Now the assertion of the theorem follows from (3.6) and (3.7). \square

Remark. Note that the asymptotic value z of \mathbf{z}_α minimizes the least-squares fit

$$\|\mathbf{b} - z\mathbf{d}\|_2$$

corresponding to the fraction (1.6) for a constant volatility $\sigma = \sqrt{z}$.

Our second approach of solving (1.6) for the volatility is similar to the first, except that we rewrite (1.6) as a linear system for the vector \mathbf{z}^{-1} consisting of the reciprocals of z_{ij} . Introducing the diagonal matrix B with the vector \mathbf{b} on its diagonal we have

$$B\mathbf{z}^{-1} \approx \mathbf{d},$$

and thus can use the same technique as before to reconstruct \mathbf{z}^{-1} . Because of the sign changes in \mathbf{b} the matrix B is also ill-conditioned in general, but again, positive approximate solutions can be obtained from the regularized problem

$$(B^2 + \beta L^T L)\mathbf{z}^{-1} = B\mathbf{d} \quad (3.8)$$

with the same matrix L of (3.4) and sufficiently large regularization parameter $\beta > 0$. With this approach, Theorem 1 yields another asymptotic volatility as $\beta \rightarrow \infty$, which minimizes the corresponding least-squares fit

$$\|\mathbf{d} - \frac{1}{z}\mathbf{b}\|_2$$

over all constant volatilities $\sigma = \sqrt{z}$.

4 Numerical results

We now present numerical reconstructions of certain volatility functions using the two approaches (3.3) and (3.8) from the previous section. Our results include first a set of synthetic data with random errors on top of them, second, the S&P500 data set from Figure 2, and third, another slightly larger S&P500 data set.

To begin with we show numerical results for synthetic data which have been generated by numerically solving the Focker-Planck equation (1.4) with the volatility phantom shown in Figure 4. The option prices have been sampled on the same grid as in Figure 1, and random errors have been added on top of them to achieve a total relative error of 1% in the Euclidean norm. Afterwards these data have been differentiated numerically with the very scheme of Section 2. Numerical reconstructions on the basis of (3.3) and (3.8), respectively, are shown in Figure 5, using optimized regularization parameters of the form $10^{\nu/2}$ with integers ν . As can be seen the characteristic features of the reconstructions match very well with those of the true phantom, although, of course, there are some differences in the details due to the ill-posedness of the problem.

Next, we turn to the S&P500 data set shown in Figure 2. Corresponding reconstructions of the volatility can be seen in Figure 6. While these two reconstructions agree pretty much qualitatively, the solution of (3.8) is consistently about 0.01 larger than the other one. This is in agreement with the asymptotic constant volatilities of Theorem 1 which in this example turn out to be $\sigma = 0.1531$ for (3.3) and $\sigma = 0.1676$ for (3.8), respectively.

For this real data set the choice of the regularization parameters is more subtle than before, because the exact solution is not known. Unfortunately, standard parameter choice criterions (as suggested for example in [3]) are not really useful here. In our implementation we solve this problem by determining the smallest parameter $\alpha_* = 10^{\nu/2}$ (resp. β_*) with integer ν , which yields a positive solution vector. Then, enlarging this regularization parameter by an extra factor of 100 or so appears to give good results, in that the ‘volatility smile’ looks most reasonable (visually).

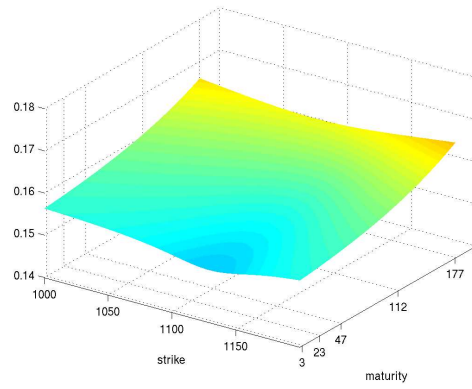


Figure 4: Volatility phantom used to generate synthetic data

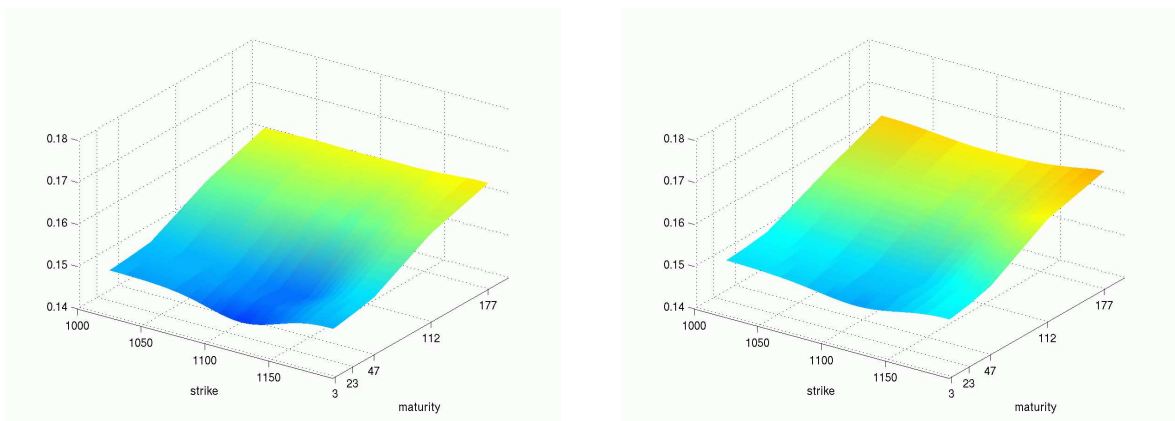


Figure 5: Reconstructions of the volatility phantom using (3.3), left, and (3.8), right

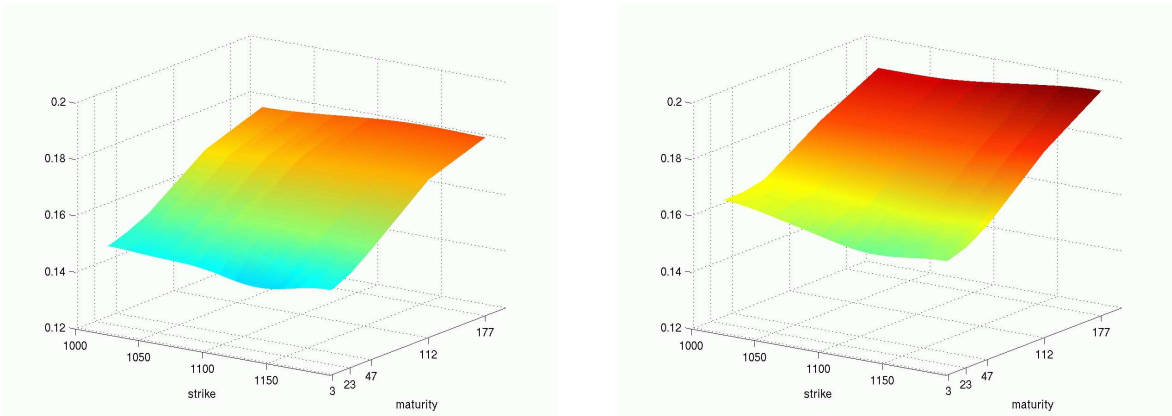


Figure 6: Reconstructions of an unknown volatility function using (3.3), left, and (3.8), right

The resulting parameters, $\alpha = 10^{11}$ and $\beta = 10^3$, are close to those of the synthetic data set above and appear to be huge. However, they have to be put in relation to the spectral norms of L , D and B , namely

$$\|L\|_2^2 \approx 4, \quad \|D\|_2^2 \approx 2 \cdot 10^8, \quad \|B\|_2^2 \approx 0.5.$$

Taking also the squared condition number of L into account (which is close to 10^5), the orders of magnitude of the two regularization parameters make sense.

As yet another example we finally have run our code with option prices for the S&P500 index from June 6, 2001, which is a somewhat larger data set than the one from our first example. The performance of our algorithm, however, is very alike: Figure 7 shows the result of the smooth interpolation, and Figure 8 the corresponding reconstructions of the volatility function. The same regularization parameters as before turn out to give best results, and again, the volatility computed from (3.8) is somewhat larger than the other one.

We mention that the amount of work for solving the inverse problem by the approach described in this paper is dominated by the solution of the regularized linear systems (3.3) and (3.8), respectively, using a sequence of up to 20 regularization parameters, say. These linear systems are sparse with, e.g., 2256 unknowns z_{ij} for the second (larger) data set. Using MATLAB [8] the solution of one such system takes about 0.1 seconds on an Intel Pentium IV processor with 1.5 GHz. This is much cheaper than solving the diffusion equations (1.2) or (1.4) for one single volatility, the latter being the basic ingredient of any output least squares type method.

We finally mention that the number of unknowns that are actually used to set up the linear systems depends on the range of available strikes and maturities. If this number is significantly larger than above, iterative methods for solving the linear systems can provide a worthwhile alternative.

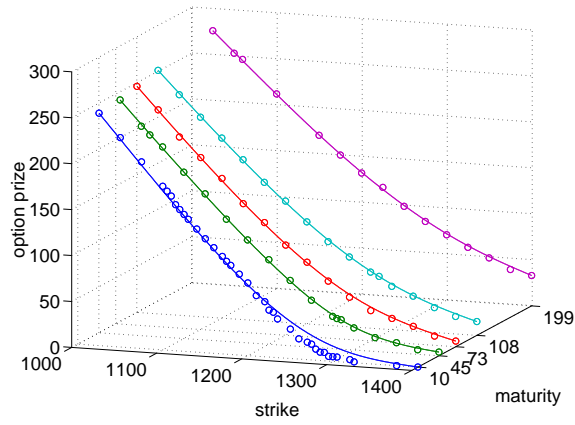


Figure 7: Smooth interpolation of the S&P500 data from June 6, 2001

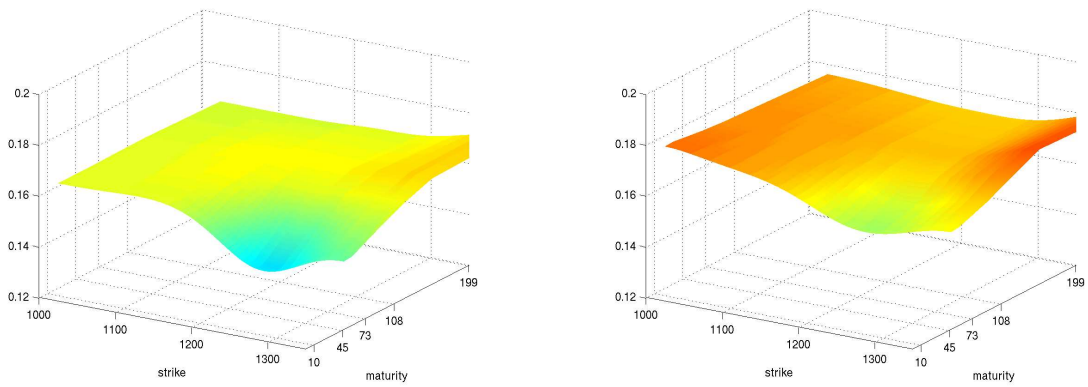


Figure 8: Reconstructions of the unknown volatility function corresponding to the data in Figure 7.

References

- [1] S. Crépey. Calibration of the local volatility in a trinomial tree using Tikhonov regularization. *Inverse Problems*, 19:91–127, 2003.
- [2] B. Dupire. Pricing with a smile. *Risk*, 7:18–20, 1994.
- [3] H. W. Engl, M. Hanke, and A. Neubauer. *Regularization of Inverse Problems*. Kluwer Academic Publishers, Dordrecht, 1996.
- [4] H. W. Engl and W. Rundell, editors. *Inverse Problems in Diffusion Processes: Proceedings of the GAMM-SIAM Symposium*. SIAM, 1995.
- [5] G. H. Golub and C. F. Van Loan. *Matrix Computations*. The Johns Hopkins University Press, Baltimore, London, 1996.
- [6] M. Hanke and O. Scherzer. Error analysis of an equation error method for the identification of the diffusion coefficient in a quasilinear parabolic differential equation. *SIAM J. Appl. Math.*, 59:1012–1027, 1999.
- [7] M. Hanke and O. Scherzer. Inverse problems light: Numerical differentiation. *Amer. Math. Monthly*, 108:512–521, 2001.
- [8] The MathWorks. <http://www.mathworks.com>.
- [9] PMPublishing. <http://www.pmpublishing.com/volatility/sp.html>.
- [10] C. H. Reinsch. Smoothing by spline functions. *Numerische Mathematik*, 10:177–183, 1967.